JBC Papers in Press. Published on March 14, 2019 as Manuscript RA118.005411
The latest version is at http://www.jbc.org/cgi/doi/10.1074/jbc.RA118.005411

Ethanol sensitizes skeletal muscle to ammonia-induced molecular perturbations

Sashi Kant[1], Gangarao Davuluri[1€], Khaled A. Alchirazi[1,] Nicole Welch[1], Claire Heit[2], Avinash Kumar[1], Mahesha Gangadhariah[1], Adam Kim[1], Megan R. McMullen[1], Belinda Willard[3], Donal S. Luse[4], Laura E. Nagy[1], Vasilis Vasiliou[5], Anna Maria Marini[6], David Weiner[7,8], Srinivasan Dasarathy[1,9*]

[1]Departments of Inflammation and Immunity and [9]Gastroenterology, Cleveland Clinic, Cleveland, Ohio, USA; [2]Department of Pharmaceutical Sciences, School of Pharmacy, University of Colorado Anschutz Medical Campus, Aurora, Colorado, USA; [3]Metabolomic and Proteomics core, Cleveland Clinic, Cleveland, Ohio; [4]Department of Cardiovascular and Metabolic Sciences, Cleveland Clinic, Cleveland, Ohio, USA; [5]Department of Environmental Health Sciences, Yale School of Public Health, New Haven, Connecticut, USA; [6] Biology of Membrane Transport Laboratory, Department of Molecular biology, Institut de Biologie et de Médecine Moléculaires (IBMM), Université Libre de Bruxelles CP300, Belgium; [7]Division of Nephrology, Hypertension, and Renal Transplantation, Department of Medicine in the School of Medicine, University of Florida, Gainesville, Florida, USA; [8]Nephrology and Hypertension section, North Florida/South Georgia Veterans Health System, Gainesville, Florida, USA.

Running title: Ethanol aggravates hyperammonemia

[€]Present address: Integrated Physiology and Molecular Metabolism, Pennington Biomedical Research Center, Baton Rouge, Louisiana, USA

*****To whom correspondence should be addressed: Srinivasan Dasarathy MD, NE4 208, Lerner Research Institute, 9500 Euclid Avenue, Cleveland, Ohio 44195; Email: dasaras@ccf.org, Tel: 2164442980, Fax: 2164453889

Key words: RhBG, proteostasis, signaling, autophagy, sarcopenia

ABSTRACT

Ethanol causes dysregulated muscle protein homeostasis while simultaneously causing hepatocyte injury. Since hepatocytes are the primary site for physiological disposal of ammonia, a cytotoxic cellular metabolite generated during a number of metabolic processes, we determined if hyperammonemia aggravates ethanol-induced muscle loss. Differentiated murine C2C12 myotubes, skeletal muscle from pair-fed or ethanol-treated mice and human patients with alcoholic cirrhosis and healthy controls were used to quantify protein synthesis, mTORC1 signaling and autophagy makers. Alcohol metabolizing enzyme expression and activity in mouse muscle and myotubes and ureagenesis in hepatocytes were quantified. Expression and regulation of the ammonia transporters, RhBG and RhCG, were quantified by real time PCR, immunoblots, reporter assays, biotin tagged promoter pulldown with proteomics, and loss of function studies. Alcohol and aldehyde dehydrogenases were expressed and active in myotubes. Ethanol exposure impaired hepatocyte ureagenesis, induced muscle RhBG expression and elevated muscle ammonia concentrations. Simultaneous ethanol and ammonia treatment impaired protein synthesis and mTORC1 signaling and increased autophagy with consequent decreased myotube diameter to a greater extent than either treatment alone. Ethanol treatment and withdrawal followed by ammonia exposure resulted in greater impairment in muscle signaling and protein synthesis than ammonia treatment in ethanol-naïve myotubes. Of the 3 transcription factors that were bound to the RhBG promoter in response to ethanol and ammonia, DR1/NC2 indirectly regulated transcription of RhBG during ethanol and ammonia treatment. Direct

effects of ethanol was synergistic with increased ammonia uptake in causing dysregulated skeletal muscle proteostasis and signaling perturbations with a more severe sarcopenic phenotype.

Skeletal muscle loss is a consistent manifestation of chronic alcohol use and in patients with alcoholic liver disease (ALD) (1-3). Clinical observations have suggested a more severe phenotype of skeletal muscle loss with ALD than in non-alcoholic liver disease but the mechanistic basis of these observations is not known (1). We and others have reported impaired muscle protein synthesis and increased autophagy and unaltered proteasome mediated proteolysis by ethanol (4-14). It is believed that the adverse consequences are primarily due to direct ethanol mediated effects on the skeletal muscle with circulating acetaldehyde from hepatic metabolism of ethanol contributing to dysregulated proteostasis in the skeletal muscle (4,11,15-17). Even though ethanol is metabolized in a number of organs, it is not known if ethanol is directly metabolized in the skeletal muscle and the acetaldehyde generated locally contributes to the perturbed proteostasis (18,19). Myotubes treated with ethanol alone as well in combination with chemical inhibitors of alcohol and acetaldehyde dehydrogenase demonstrated increased autophagy by acetaldehyde (4). These data suggest but do not directly show that ethanol is metabolized in the skeletal muscle. It is not known if alcohol and acetaldehyde dehydrogenase expression or activity occurs in the muscle of mammals. To determine this, we quantified the expression of ethanol metabolizing enzymes and their activity in skeletal muscle from ethanol treated mice as well as murine myotubes and studied their responses to ethanol exposure.

In addition to ethanol-induced changes in proteostasis, ethanol also causes hepatocellular dysfunction with impaired ureagenesis (20-23). Impaired ureagenesis results in hyperammonemia in liver disease (24-26). It is not known if hepatic ureagenesis is impaired in response to ethanol or its metabolite, acetaldehyde, but there is emerging data that acetaldehyde impairs hepatic ureagenesis (27). During hepatocellular dysfunction and hyperammonemia, the skeletal muscle becomes a metabolic partner to the liver with increased muscle uptake of ammonia (28-30). This is relevant because hyperammonemia results in dysregulated skeletal muscle proteostasis with impaired protein synthesis and increased autophagy and consequent sarcopenia (28,31-36). These data suggest that, in addition to the direct effects of ethanol or acetaldehyde on muscle proteostasis, increased muscle ammonia uptake can perturb the molecular and metabolic responses with muscle loss. Expression of the RhBG ammonia transport protein has been reported in the skeletal muscle suggesting its involvement in muscle ammonia uptake.(37,38) Limited data are available on the regulation of RhBG expression in the skeletal muscle. Additionally, in patients with alcoholic liver disease, muscle loss persists even after stopping drinking that may be due to persistent hepatocyte dysfunction and hyperammonemia. Whether prior ethanol exposure sensitizes the skeletal muscle to hyperammonemia of the underlying liver disease is a clinically relevant mechanistic question. To address this, we evaluated proteostasis and signaling responses in ethanol myotubes pretreated with ethanol followed by ethanol withdrawal and subsequent ammonia treatment. Finally, we also tested if ethanol directly alters skeletal muscle ammonia uptake and alters the expression of the RhBG ammonia transporter.

In the present studies, we determined protein synthesis and autophagy markers in myotubes in response to ethanol, ammonium acetate, ethanol pretreatment followed by ammonium acetate, and combined ethanol and ammonium acetate treatment. Since translational control in protein homeostasis is critical for cellular function (39), a number of signaling pathways intersect at multiple regulatory levels. Therefore, focusing on a single regulatory pathway may not provide true mechanistic insights into the responses observed with interventions that alter muscle protein homeostasis. Critical regulators of muscle proteostasis include mTORC1 signaling (increases protein synthesis) and phosphorylation of the α subunit of eukaryotic initiation factor 2 (decreases protein synthesis) (28), both of which were quantified in myotubes

and muscle tissue. We also quantified skeletal muscle alcohol and acetaldehyde dehydrogenase activity in myotubes and skeletal muscle from ethanol-fed mice because it is not yet known if ethanol metabolizing enzymes are expressed and are active in the muscle tissue and ethanol metabolism in the muscle can generate cytotoxic acetaldehyde locally. Finally using RhBG luciferase reporters including full length and deletional constructs, we determined the regulation of the ammonia transporter in response to ethanol, ammonia and both in combination. We also sought to identify the mechanistic basis for more severe muscle loss with ethanol exposure and determined if ethanol or its metabolite, acetaldehyde directly reduce muscle loss and additionally, via impaired ureagenesis in the liver, aggravate signaling and protein synthesis via hyperammonemia, a known mediator of the liver-muscle axis. Finally, even though RhBG is a TATA-less promoter, using a promoter pulldown with proteomics to identify transcription factors that bind to the RhBG promoter we noted that downregulation of transcription/negative control 2 (DR1/NC2) indirectly regulated RhBG transcription in response to ethanol and ammonia in the muscle.

Results

Ethanol impairs ureagenesis in hepatocytes and results in more severe muscle hyperammonemia

In murine primary hepatocytes, ethanol exposure resulted in decreased urea synthesis measured by urea concentrations in the medium (**Fig. 1, A**). Since ureagenesis in the hepatocytes is the major mechanism of ammonia metabolism, ammonia concentrations in the medium in response to ethanol was higher than in the medium from untreated controls. (**Fig. 1, B**). In AML12 cell lines, lower urea and higher ammonia concentrations were noted in response to ethanol treatment compared with controls (**Supplementary Fig. 1, A, B**). However, in contrast to the response in primary hepatocytes, ureagenesis by AML12 was lower. We also observed that ammonia concentration in ethanol treated myotubes and in the plasma and skeletal muscle of mice exposed to ethanol was significantly higher ($p<0.001$) compared with appropriate controls (**Fig. 1, C**). To determine how ethanol exposure and hyperammonemia cause an increase in muscle ammonia concentrations, we determined the expression of ammonia transporters, RhBG and RhCG mRNA and protein in myotubes and skeletal muscle from mice and human subjects.

Ethanol and hyperammonemia independently upregulate skeletal muscle RhBG ammonia transporter expression

Ethanol treatment and hyperammonemia independently increased ammonia transporter, RhBG protein and mRNA expression but not RhCG protein in myotubes (**Fig. 2, A, B**). A combination of ethanol and hyperammonemia also increased the expression of RhBG protein but ethanol withdrawal followed by ammonia resulted in an even greater increase in RhBG expression (**Fig. 2, C**). Skeletal muscle from ethanol fed or ammonia treated mice and human cirrhotic patients also showed increased expression of RhBG mRNA and protein but not RhCG in skeletal muscle compared to that in muscle from controls (**Fig. 2, D, E**).

Consistently, reporter assay for RhBG showed that both ethanol and ammonia increased luciferase activity in myotubes (**Fig. 3, A**). Interestingly, the combination of ethanol and ammonia resulted in greater luciferase reporter activity than either alone (**Fig. 3, A**). Both ethanol and its key toxic metabolite, acetaldehyde, increased RhBG promoter activity **(Fig. 3. B)**. Consistent with our previous work that blocking the metabolism of ethanol using 4-methylpyrazole or acetaldehyde metabolism with cyanamide increased autophagy in myotubes, we also observed that both ethanol and acetaldehyde increased the ammonia transporter, RhBG reporter activity **(Fig. 3. C, D)**. Interestingly, we did not observe a similar increase in expression of RhBG protein in primary hepatocytes or AML12 cells in response to ethanol treatment (**Supplementary Fig. 1, C**).

Transfection of previously published full length and deletional constructs of RhBG luciferase reporter (**Fig. 4, A**) (40) in murine myotubes showed that, similar to that in HepG2 cells, deletion upstream of 22 bp from the transcription start site resulted in loss of reporter activity. However, unlike that in HepG2 cells (40), deletion from -180 to -1499 resulted in

attenuation of the reporter activity but reporter activity increased in the constructs between -60 to -120 bp upstream of the TSS compared to the full length promoter construct (**Fig. 4, D**). These suggested possible context specific repressors or enhancers specific to the skeletal muscle. Biotin tagged promoter pulldown of DNA binding proteins (**Supplementary Table 1**) were then analyzed for transcription factors that were bound to the promoter. Of a total of 17 transcription factors that were bound in response to either hyperammonemia or ethanol exposure, 3 factors were identified that were bound to the RhBG promoter under all conditions (**Fig. 4, B**) and included FoxPI, PBX1 and the general transcriptional repressor, DR1/NC2. Analysis of the known RhBG promoter sequence showed multiple binding sites for FoxP1 and PBX1 with high level of confidence ($p<0.001$ cutoff). (**Fig. 4, C**). Since DR1/NC2 does not bind directly to promoters (41,42), consensus sites for DR1/NC2 binding have not been identified but DR1/NC2 dependent transcriptional regulation is mediated via TATA binding proteins or other binding partners. Even though RhBG is a TATA-less promoter (40) and DR1/NC2 was initially identified to repress transcription of genes with TATA box containing promoters (41,42), subsequent investigations showed that DR1/NC2 can repress genes with TATA-less promoters (43). While RhBG does not have a canonical element, it does have a TGAAA (at -30 from the TSS), that is a TATA like element. These are much more frequent than canonical TATA elements and could be responsible for mediating the DR1/NC2 effects. Based on the putative binding sites of the 2 transcription factors identified to bind to the RhBG promoter, we used our reporter constructs to determine the response to ethanol, ammonia and a combination of ethanol and ammonia (**Fig. 4, D**). Compared to untreated control cells, the full length reporter showed increased luciferase activity in response to hyperammonemia, ethanol or a combination of ethanol and ammonia. However, with sequential deletion on the full length promoter upstream of the transcription start site, there was a reduction in luciferase activity (-1499 to -240) followed by an increase in luciferase activity in response to the interventions with a marked reduction in luciferase activity in the construct with only 22 bp upstream of the TSS. However, with the intervention, from -1499 to -180, there was increased luciferase activity compared to the response in the untreated control cells. Further deletion of promoter sites resulted in an increase in luciferase activity but there was limited to no response to the interventions. These suggest that regulation by ammonia or ethanol occur at the sites from -1499 to -180 from the TSS on the RhBG promoter. Complementary studies using genetic depletion of the transcription factors were then performed with significant silencing efficiency (**Fig. 4, E**). Depletion of DR1/NC2 and PBX1 resulted in an increase in luciferase activity in the untreated cells, suggesting that they functioned as repressors for promoter activity (**Fig. 4, F**). We noted that depletion of negative regulator of transcription, DR1/NC2 depletion resulted in loss of response to ammonia or ethanol while PBX1 depletion resulted in continued response, albeit at a higher basal activity in response to the interventions. Finally, depletion of FoxP1 did not affect either baseline response in untreated cells or the response to interventions and was similar to that observed with myotubes transfected with a random construct. These data suggested that DR1/NC2 regulated RhBG promoter activity. Our observations of an increased RhBG expression and reporter activity of the TATA less promoter suggested that ethanol and ammonia regulate RhBG potentially by inhibiting RhBG repressors. This interpretation is consistent with the responses to ethanol and ammonia in the deletional constructs.

Having identified putative binding sites and responses in promoter constructs and reporters, expression of the transcription factors was quantified by immunoblots. Expression of DR1 and FoxP1 were increased in whole cell lysates while PBX1 was unaltered in response to the interventions. Given the consistency in binding of DR1/NC2 to the promoter, increased expression of DR1 and FoxP1 during hyperammonemia and ethanol with ammonia was noted (**Fig. 5, A, B**) while PBX1 expression was unchanged in response to the interventions (**Fig. 5, C**). Even though DR1/NC2 is a negative regulator of transcription, we investigated if depletion of the general

transcriptional repressor, DR1/NC2 alters RhBG expression (**Fig. 5, D**). DR1/NC2 depletion resulted in only a mild increase in RhBG protein expression. However, consistent with the reporter activity data, depletion of DR1/NC2 resulted in loss of response to interventions. Interestingly, PBX1 depletion also increased baseline luciferase activity of the reporter for RhBG promoter but the responses to ethanol and ammonia were maintained suggesting that PBX1 may negatively regulate the RhBG promoter and the maintenance of responses to ethanol and ammonia despite depletion of PBX1 suggested that the increased RhBG was independent of this transcription factor. We then tested if skeletal muscle hyperammonemia during ethanol exposure worsened the sarcopenic phenotype and dysregulated proteostasis by quantifying the myotube diameter, protein synthesis and autophagy markers in myotubes.

Ethanol-induced reduction in myotube diameter and proteostasis were worsened by ammonia

Myotube diameter and protein synthesis in myotubes were significantly decreased, and autophagy markers showed increased expression in response to ethanol exposure for 6h and 24h (**Fig. 6, A-C; Supplementary Fig. 2**). Consistent with our previous reports, ammonia exposure resulted in reduced protein synthesis, increased autophagy markers and lower myotube diameter all of which are characteristics of a sarcopenic phenotype in myotubes (29,36). A combination of ethanol and ammonium acetate resulted in greater reduction in myotube diameter and protein synthesis and increased autophagy markers than either ethanol or ammonium acetate alone. Finally, ethanol withdrawal followed by ammonia exposure resulted in greater impairment of protein synthesis and increased autophagy markers than either treatment alone (**Fig. 6, C**).

Regulation of muscle proteostasis is regulated by multiple regulatory molecules including TGFβ superfamily member, myostatin, its downstream target AMPK and mTORC1 and phosphorylation of eIF2α(28). Even though specific perturbations in regulation of each of these molecules have been reported to result in a sarcopenic phenotype, we determined the alterations in expression of the regulatory components of this integrated pathway of muscle proteostasis. Since mTORC1 is a critical regulator of proteostasis, and muscle hyperammonemia occurs during and after ethanol exposure, we determined the perturbations in signaling pathways altered by hyperammonemia, ethanol treatment and hyperammonemia following ethanol exposure.

Perturbations in signaling pathways were more severe with hyperammonemia following ethanol exposure

Consistent with a more severe phenotype of reduced myotube diameter and dysregulated proteostasis with ethanol and hyperammonemia, mTOR phosphorylation and mTORC1 signaling determined by phosphorylation of P70S6 kinase and ribosomal S6 protein were impaired by ethanol and ammonia at 6h with greater impairment at 24h. Similar observations were noted in myotubes treated with simultaneous ethanol and hyperammonemia and ethanol treatment followed by hyperammonemia also resulted in impaired mTOR phosphorylation and mTORC1 signaling (**Fig. 7**). Since ethanol and ammonia induce cellular stress and inhibit protein synthesis via phosphorylation of eIF2α with global repression of mRNA translation and protein synthesis as well as inhibiting mTORC1 signaling, we then tested if eIF2α phosphorylation occurs during ethanol and ammonia exposure.

Phosphorylated eIF2α (eIF2α-P) expression was increased in myotubes during ethanol or ammonia treatment and to a greater extent with both ethanol and ammonia (**Fig. 8, A**). Ethanol withdrawal followed by hyperammonemia increased eIF2α-P. Of the eIF2α kinases in the skeletal muscle, GCN2 phosphorylation and activation was observed with both ethanol and hyperammonemia, but to a greater extent in response to simultaneous ethanol treatment and hyperammonemia. Ethanol withdrawal followed by hyperammonemia also resulted in significantly higher GCN2 activation compared to either treatment alone. The other eIF2α kinase, protein kinase R like endoplasmic reticulum kinase

(PERK) was not activated as noted by the lack of mobility shift in response to ethanol, hyperammonemia, a combination of the two or hyperammonemia following ethanol withdrawal (**Fig. 8, A**). Increased eIF2α-P and GCN2 phosphorylation without PERK activation were also observed in pair- or ethanol-fed mice and human alcoholic cirrhosis and controls (**Fig. 8, B**).

In addition to the cellular stress response, myostatin is another known inhibitor of protein synthesis and muscle loss. Expression of myostatin was increased by ethanol treatment, hyperammonemia and a combination of ethanol and hyperammonemia (**Fig. 8, C**). However, phosphorylation of AMPK, a downstream target of myostatin was increased with ammonia exposure and ethanol withdrawal followed by ammonia exposure but not with ethanol alone or ethanol in combination with ammonia (**Fig. 8, C**). Finally, even though ethanol-induced perturbations were identified in multiple systems, whether ethanol is metabolized in the myotubes is currently unknown.

Ethanol is directly metabolized in the skeletal muscle

In addition to the direct effects of ethanol on the muscle as observed with the use of 4- methylpyrazole, an ADH inhibitor, ADH and ALDH enzyme activity was noted in murine myotubes and skeletal muscle from mice acutely or chronically treated with ethanol suggesting that ethanol was directly metabolized in the muscle **(Fig. 9, A-D).** Transcriptional expression of ADH3 and ALDH2 were increased in the skeletal muscle in response to ethanol exposure **(Supplemental Fig. 3)**.

Activity of both ADH and ALDH enzymes were acutely inhibited in myotubes and returned to basal activity after 3h in response to ethanol while ammonia exposure increased the activity of ADH.

Discussion

We show that ethanol-induced dysregulated skeletal muscle proteostasis, signaling perturbations and sarcopenia phenotype is due to ethanol as well as hyperammonemia in a comprehensive array of models including human muscle, ethanol treated mice and myotubes. Both ethanol and ammonia upregulated transcription and protein expression of the ammonia transporter, RhBG, in the skeletal muscle with increased tissue concentration of ammonia. We also identified that general transcriptional repressor, DR1/NC2 indirectly regulates the promoter activity of RhBG. Ethanol induced perturbations in ammonia metabolism results in perturbations in the major signaling pathways that regulate muscle protein homeostasis and result in a sarcopenic phenotype.

Our in vitro studies in primary hepatocytes and AML12 murine liver cell lines show that ethanol impaired hepatocyte ammonia disposal due to decreased ureagenesis, and is consistent with previous *in vivo* studies (20-23,27,44). We and others have also previously reported that the skeletal muscle functions as a metabolic partner to the liver during impaired ureagenesis by increased muscle uptake of ammonia (28,29). Lower ureagenesis results in impaired hepatic ammonia disposal and the resultant hyperammonemia results in increased skeletal muscle ammonia concentrations as observed in the present studies in skeletal muscle from ethanol fed mice with consequent ammonia mediated effects as reported earlier (28-30).

The present studies provide a mechanistic basis for increased muscle uptake of ammonia in response to ethanol exposure. Expression of ammonia transporter family member, RhBG, is transcriptionally upregulated in the skeletal muscle during ethanol exposure. Expression of another ammonia transporter family member, RhCG, is however not significantly altered in the muscle either with ethanol or hyperammonemia. Of the 3 transcription factors that were bound to the RhBG promoter during ammonia and ethanol exposure, only DR1/NC2 and FoxP1 were increased in response to ethanol and ammonia unlike PBX1 whose expression was unaltered with these interventions. Depletion of either DR1/NC2 or PBX1 increased the luciferase reporter activity for the RhBG promoter suggesting that both these transcription factors negatively regulated RhBG. However, depleting PBX1 did not alter the response to ethanol or ammonia while DR1/NC2 depletion resulted in a

loss of response to ethanol and ammonia showing a regulatory role for DR1/NC2 in ammonia/ethanol mediated regulation of RhBG. Maintenance of luciferase response to ammonia and ethanol despite depletion of PBX1 or FoxP1 suggested that RhBG regulation was independent of these 2 transcription factors. Even though DR1/NC2 is a repressor of transcription, our studies on the expression and loss of function studies suggest that DR1/NC2 may be an indirect regulator of RhBG by inhibiting an RhBG repressor. This interpretation is supported by our observations on reporters of deletional constructs of the RhBG promoter. Our data on the pulldown proteomics, luciferase reporter assays and depletion studies are consistent with the known function of DR1/NC2 as a transcriptional repressor. However, the expression of RhBG protein does not show a similar robust response and lack of response to ammonia or ethanol exposure. Whether these depend on regulation via TATA like rather than TATA element on the promoter or post transcriptional or translational responses need further evaluation as part of future studies.

We also noted that ethanol is metabolized in the skeletal muscle and inhibition of ethanol or acetaldehyde metabolism showed that blocking ethanol oxidation results in a prolonged increase in RhBG expression while inhibiting acetaldehyde oxidation with cyanamide results in a rapid and early rise in RhBG expression. These data suggest that ethanol and acetaldehyde increase ammonia transporter and transport with different kinetics.

Published data show that ethanol and hyperammonemia cause skeletal muscle loss and decreased myotube diameter (4,11,45,46). Our current observations on signaling perturbation in response to ethanol exposure are consistent with prior reports of ethanol mediated impairment in skeletal muscle mTORC1 signaling and protein synthesis and increased autophagy *in vitro* and *in vivo* in mouse models (4,47). Our observations that phosphorylation of AMPK, an upstream inhibitor of mTOR phosphorylation and activator of autophagy, by ethanol treatment with or without hyperammonemia was less than that observed with hyperammonemia alone and may be due to dephosphorylation of AMPK in response to ethanol as has been reported in hepatocytes but different from that reported in myoblasts (48,49). These suggest that the effects of ethanol on signaling perturbations may be context dependent and therapeutic approaches need to consider these tissue specific responses. Our signaling data also provide a mechanistic explanation for the clinical observation of more severe muscle loss in patients with alcoholic liver disease with impaired mTORC1 signaling and increased eIF2α-P that is greater in myotubes during hyperammonemia with ethanol treatment. Increasing recognition that eIF2α-P impairs mTORC1 signaling suggests a similar mechanism in myotubes treated with ethanol and ammonia (33). Increased myostatin expression at 6 and 24 h in response to ethanol exposure and hyperammonemia are consistent with our previous reports of hyperammonemia-induced upregulation of myostatin (29). As mentioned earlier, perturbations in multiple regulatory pathways include adaptive and maladaptive responses that culminate in dysregulated protein homeostasis and a sarcopenic phenotype.

Our data show that dysregulated proteostasis during ethanol exposure is mediated by transcriptional and signaling perturbations at multiple levels. Both ethanol directly and muscle generated acetaldehyde and possibly systemic acetaldehyde impair protein synthesis, increase autophagy and consequent sarcopenia. Additionally, impaired ammonia disposal due to ethanol mediated decreased hepatic ureagenesis causes dysregulated proteostasis. Importantly, even after ethanol withdrawal, once liver disease is established the resultant hyperammonemia maintains and worsens dysregulated protein homeostasis. This can explain the persistent muscle loss in human patients in contrast to a reversible phenotype of muscle loss in rodents because hepatic fibrosis and cirrhosis do not occur in these models. Ammonia lowering therapy reverses muscle loss in preclinical models of hyperammonemia (31) abstinence in combination with ammonia lowering therapy has potential for rapid clinical translation (1,2,50).

Experimental procedure

All chemicals including ethanol, acetaldehyde, 4-methylpyrazole, and cyanamide were obtained from Sigma Aldrich (St. Louis,

MO, USA). Antibodies were obtained as follows: antipuromycin antibody from Millipore (Millipore-Sigma, Burlington, MA, USA), LC3II, and PBX1 from Novus biologicals (Littleton, CO, USA), β- actin from SantaCruz biotechnology Co. (Dallas, TX, USA), total and phosphorylated mTOR ^{Ser2448}, P70S6 kinase^{Thr389}, ribosomal S6 protein$^{Ser240/244}$, GCN2^{Thr899}, eIF2α^{Ser51}, AMPK^{Thr172}, PERK, DR1/NC2, FoxP1 and P62 from Cell Signaling Technologies (Beverly, MA, USA). Antibodies to RhBG and RhCG were generated by David Weiner (author) and have been characterized previously (51,52). shRNA clones for DR1/NC2, FoxP1 and PBX1 were obtained from Sigma-Aldrich (St. Louis, MO).

In vitro cell cultures.

Murine myotubes. Murine C2C12 myoblasts (ATCC, Manassas, VA, USA) were grown to confluence in proliferation medium (DMEM with 10% fetal bovine serum) followed by differentiation in DMEM with 2% horse serum for 48 h as previously described (36,53). Differentiated murine C2C12 myotubes exposed to 100mM ethanol with or without 10mM ammonium acetate were used for 6 and 24h and shown to be biologically and clinically relevant as reported previously (4,36). For the withdrawal experiments, myotubes were treated with 100mM ethanol in differentiation medium for 24 h after which the medium was removed and replaced with fresh conditioned differentiation medium with 10mM ammonium acetate.

Primary hepatocyte isolation. Hepatocytes from WT mice was isolated using methods previously described (54). Hepatocytes were isolated from livers perfused via the portal vein with modified Hank's solution (free of Ca^{2+} and Mg^{2+}) containing 1mM EGTA and 10mM HEPES and then with 0.05% type I collagenase in Williams' E medium at a flow rate of 6 mL/min. A cell suspension was formed by gentle disruption of the collagenase-treated livers in Williams' E medium containing 10% fetal bovine serum. Cells were washed twice with Williams' E and dead/damaged hepatocytes were separated out with a 30% Percoll gradient. Purified cells were suspended in William's E supplemented with 10% FBS and hepatocyte maintenance pack which is from Gibco (Carlsbad, CA, USA). Cells were counted, plated on collagen coated 100mm plates ($1.8x10^6$ cells per plate).

Culture and treatment of AML12 cells. AML12 mouse hepatocytes were obtained from ATCC and cultured in a 1:1 mixture of Dulbecco's modified Eagle's medium and Ham's F12 medium (Sigma Aldrich, St. Louis, MO, USA) with 1X insulin, transferrin and selenium (ThermoFisher Scientific, Waltham, MA, USA), 1X dexamethasone (Cayman Chemical, Ann Arbor, MI, USA), 10% fetal bovine serum and 1% penicillin streptomycin. Cells were subcultured at a density of 4×10^6 cells/cm^2 in a 10 cm^2 plate, 24 h later cells were treated with 100mM ethanol in serum-free DMEM/F12 +1% penicillin streptomycin for 6h. Medium was collected at timed intervals to quantify urea concentrations.

In vivo studies in ethanol-fed mice. All procedures using animals were approved by the Cleveland Clinic Institutional Animal Care and Use Committee. 8–10 weeks old female, C57BL/6J mice (Jackson Laboratory, Bar Harbor, ME) were randomized into ethanol-fed and pair-fed groups and then adapted to a control liquid diet for 2 days. Two models of ethanol feeding were used in this study. The first was chronic ethanol-induced liver injury model, in which mice in the ethanol-fed groups were allowed free access to an ethanol-diet containing 1% (vol/vol) ethanol for 2 days followed by 2% ethanol for 2 days, then 4% ethanol for 1 week, 5% for 1 week and finally 6% ethanol for an additional week. The second model was considered a binge model of ethanol exposure. Mice were allowed free access to an ethanol-diet containing 1% for 2 days, followed by 2 days at 6% ethanol. Control mice received a control pair-food diet which iso-calorically substituted maltose dextrins for ethanol. Animals were housed in the biological resource unit with a 12 h light/day cycle. After euthanasia, gastrocnemius muscle was harvested and protein extracted for immunoblots and tissue lysates for enzyme activity.

Placement of miniosmotic pump to induce hyperammonemia. Hyperammonemia was induced in C57BL/6J mice by placing an Alzet miniosmotic pump Model 2004 (Alzet, Cupertino, CA, USA). Osmotic pump implant surgery was performed using sterile aseptic techniques. Mice were placed on a heating pad to maintain normal body temperature for the duration of the surgery. Mice were anesthetized by isofluorane anesthesia. The nape of the animal was shaved with clippers and the skin cleaned with 70% ethanol. An Alzet® 3 cm/ 200µl mini- osmotic pump containing either phosphate-buffered saline (PBS), or ammonium acetate was implanted subcutaneously in 8-9 weeks old mice on back of neck. A 5–7 mm transverse incision was made and a small subdermal pocket created using a straight, long-nosed hemostat following local anesthesia using 0.25% bupivacaine. The pump was inserted with the delivery pore located anterior toward the head of the animal and the incision secured using wound clips. A dose of 2.5mmol/kg/day ammonium acetate in sterile phosphate buffered saline or vehicle alone was delivered to these animals for 4 weeks.

Human muscle tissue. Vastus lateralis muscle from alcoholic cirrhosis and matched healthy controls were obtained after institutional review board approval (IRB 10-840) and in accordance with the Declaration of Helsinki at the Cleveland Clinic. All patients provided an informed consent, in accordance with the Declaration of Helsinki, and the clinical details of these subjects have been previously reported (55).

Myotubes diameter measurement. The diameters of at least 100 myotubes from at least 3 independent experiments each were measured using ImageJ (imagej.nih.gov/ij/list.html) as described earlier (29). The mean±SD were calculated and expressed as a ratio compared to controls.

Real time PCR. Total RNA was extracted and used for real time PCR as previously described (29). In brief, total RNA from C2C12 myotubes treated with ethanol was isolated using TRI reagent (Molecular Research Center Inc., Cincinnati, OH, USA). cDNA was synthesized using avian leukemia retrovirus reverse transcriptase (BD Clontech, Mountain View, CA, USA) and real-time PCR (**Supplementary Table 2**) performed using the SYBR® fluorescence kit (Qiagen, Hilden, Germany) with Stratagene Mx3000p (Agilent Technologies, Santa Clara, CA, USA). Relative differences were normalized to the expression of β actin.

Immunoblots. Immunoblots on protein extracts were performed using protocols established in our laboratories as described earlier (33). In brief, electrophoresis of 30µg protein was performed on an 8 or 10% tris glycine gel except for LC3 lipidation where a 15% gel was used, electrotransferred to PVDF membrane, blocked with 3% bovine serum albumin or 5% fat free milk for 2 hours, incubated with primary antibody for overnight at 4ºC followed by secondary antibody for 3 hours at room temperature in the appropriate dilutions (**Supplementary Table 2**) and blots developed. Immune reactivity was detected by chemiluminescent HRP substrate (Millipore-Sigma, Burlington, MA, USA) followed by densitometry of the blots using Image J as described earlier (56).

Protein synthesis in vitro. The puromycin incorporation method was used to quantify protein synthesis in C2C12 myotubes by incubating the cells following treatment with 100mM ethanol and/or 10mM ammonium acetate or medium alone and 1µg/ml puromycin was added for 30 min. Immunoblots for puromycin incorporation were performed as described earlier (33).

Ureagenesis. To determine the impact of ethanol on hepatic ureagenesis, murine AML12 cells or primary hepatocytes were grown as described above. Upon reaching confluence, cells were treated with 100mM ethanol or no treatment and medium aspirated from 0-6 h and urea concentration in the medium quantified. Urea assay was performed using a modification of the protocol as described previously(57). The working solution consisted of 513mg/L primaquine bisphosphate, 100mg/L o-phthalaldehyde, 2.5mol/L sulfuric acid, 2.5g/L boric acid, and 0.03% Brij-35 (Sigma-Aldrich,

St. Louis, MO, USA). Urea standards were prepared in serum free DMEM. 50µl each of standards or samples were transferred to separate wells in a flat bottom 96 well plate. 200µl of freshly prepared working reagent was added, the plate gently mixed and incubated at room temperature for 1h. Readings were taken at 430 nm on a plate reader (Molecular Devices, Sunnyvale, CA, USA).

Ammonia assays. Ammonia assays were performed as described previously (29). The working reagent consist of 150mM α-KG, 2.5mM NADH and 1µg/µl of glutamate dehydrogenase enzyme. The ammonia standard was prepared from 1mM solution of ammonium chloride. To perform the assay, 60µl of culture medium was transferred to UV invisible flat bottom 96 well plate. Then 20µl of 150mM α-KG and 20µl of freshly prepared 2.5mM NADH were added. The plate was gently mixed and optical density (OD) was taken at 340 nm. Then 5µg of glutamate dehydrogenase enzyme was added to each well. The plates were kept for incubation at 37ºC for 1h in the plate reader machine. During the incubation OD was taken at every 15 min at 340 nm on the plate reader (Molecular Devices, Sunnyvale, CA, USA). During calculation initial OD was subtracted for the final OD.

Enzyme activity assays. Alcohol and aldehyde dehydrogenase assays were performed using an assay kit per manufacturer protocol (Biomedical Research Service Center, University of Buffalo, Buffalo, NY, USA). In brief, myotubes or muscle tissue was lysed using ice cold 1X lysis solution provided with kit. Cell lysates was extracted by pipetting up and down. The cell lysate was gently and intermittently agitated on ice for 5 min followed by centrifugation for 10 min at 12000 rpm at 4ºC. The supernatant was used for ADH and ALDH assay. For tissue extraction, ~50mg pair-fed and ethanol-fed mice gastrocnemius muscle tissue was taken and homogenized in 500µl ice cold 1X cell lysis solution provided with kit. The homogenates were centrifuged for 10 min at 12000 rpm at 4ºC and supernatant was harvested. Protein concentration (1mg/ml) of each sample were equalized by performing protein estimation assay (BCA). Then 10µl of each sample in duplicate was transferred to separate well of flat bottom 96 well plate (one set for control and another set for reaction). Then 50µl of control solution (1 part of H20 and 10 part of ADH/ALDH assay solution) was added to one set of wells and 50µl of reaction solution (1 part of 10X ALD/ALDH substrate and 10 part of ADH/ALDH assay solution) was added to another set of wells. The plate was gently mixed, covered and kept it for incubation for 1h at 37ºC. The reaction was stopped by adding 50µl of 3% Acetic acid. Optical density (OD) was taken at 492 nm on the plate reader (Molecular Devices, Sunnyvale, CA, USA). The OD of control well was subtracted from OD of reaction well for each sample. The subtracted sample OD reading was used to calculate enzyme activity. Sample ADH/ALDH activity in IU/L unit = µmol/(L.min) = OD x 1000 x 110µl / (60 min x 0.6 cm x 18 x 10µl).

Reporter assay. To determine if ethanol resulted in transcriptional upregulation of RhBG, the previously described full length and various deletion constructs of RhBG used to generate luciferase reporters and Renilla constructs (40) were transfected in myoblasts using protocols described by us (29), cells selected using neomycin and grown in differentiation medium for 48 hours. Myotubes were treated with 100mM ethanol with or without ammonium acetate for 24 hours.

Biotin tagged promoter pulldown assay to detect transcription factor binding. RhBG full length promoter (-2349 to 142) was amplified using 5' biotin tagged forward primer and reverse primer. Biotin tagged RhBG promoter was gel purified using QIAquick gel extraction kit (Qiagen). Then, C2C12 cell lysate was made in the lysis/binding buffer (25mM Tris pH 7.5, 150mM NaCl, 0.3% Triton X-100, 1X protease inhibitor cocktail). The streptavidin magnetic beads (50µl) were pre-washed with binding buffer for three times and then 300 ng of biotin tagged RhBG promoter was added to bind with streptavidin. The beads were again washed for two times to remove unbound RhBG promoter. The binding reaction was performed by adding 100µg of C2C12 crude lysate to the biotin-

RhBG-streptavidin complex and kept at 4ºC for 4 hours at rotation. The beads were washed three times with the binding buffer and then interacting proteins were eluted by using 100µl of elution buffer (0.1M Glycine, pH 2.0). The eluted proteins were subjected to liquid chromatography mass spectrometry (LC-MS/MS) to identify proteins that interact with RhBG promoter. Protein samples were prepared for mass spectrometry by removing an aliquot of protein and reconstituting in a 50µl of 6M urea, 100mM Tris buffer. The proteins were reduced with 10mM DTT for 15 minutes at room temperature and alkylated with 30mM iodoacetamide for 20 minutes at room temperature. The samples were diluted to reduce the urea concentration to < 1.2M. Two rounds of tryptic digestion were performed by the addition of 1µg of trypsin and incubated at room temperature overnight followed by the addition of a second trypsin aliquot and digestion for an additional 4 hours. The peptide samples were desalted with PepClean C-18 spin columns (Thermo Scientific, Waltham MA, CA) and reconstituted in 30µl 1% acetic acid for LC-MS analysis.

The LC-MS system was a ThermoScientific Fusion Lumos hybrid mass spectrometry System (ThermoScientific, San Jose, CA). The HPLC column was a Dionex 15 cm x 75 µm internal diameter Acclaim Pepmap C18, 2µm, 100Å reversed- phase capillary chromatography column (Thermo Fisher, Waltham, MA). Five µL volumes of the extract were injected and the peptides eluted from the column by an acetonitrile/0.1% formic acid gradient at a flow rate of 0.3µL/min were introduced into the source of the mass spectrometer on-line. The microelectrospray ion source is operated at 1.9kV. The acquisition method was a data dependent based MS^2 method. It begins with a MS full scan in the Orbitrap analyzer (60k resolution), followed by selection of the parent ions in the MS scans and fragmentation by high energy collision induced dissociation (HCD) and detected in the Orbitrap analyzer.

The data were analyzed using MaxQuant V1.5.2.8 with the search engine Andromeda which is integrated in MaxQuant software and the parameters used were default settings for an Orbitrap (58,59). The database used to search the MS/MS spectra was the Uniprot mouse protein database (https://www.uniprot.org/proteomes/UP000000589) containing 25,035 entries with an automatically generated decoy database (reversed sequences). Oxidation of Methionine and acetylation of protein N-terminus were set as dynamic modifications and carbamidomethylation of Cysteine was set as static modifications. A false discovery rate (FDR) was set to 1% for both peptide and protein with a minimum length of seven amino acids, two unique or razor peptides were required for positive identification.

The "match between runs" feature of MaxQuant was used to transfer identifications to other LC-MS/MS runs based on their masses and retention time (maximum deviation 0.7 min) and this was also used in quantification experiments. Quantifications were performed with the label-free quantitation method available in the MaxQuant program(60).

After mass spectrometric analyses (peptide/protein identification, LFQ intensity calculations, and normalization), we selected all known transcription factors, and removed all proteins that were bound to beads in the no DNA control as background. The search motif tool in the eukaryotic promoter database (EPD) scans promoter regions with position weight matrices (PWM) of several transcription factors (TF) and core promoter elements to find putative binding sites. Once a PWM library and TF were selected, the identified promoter region was searched with that PWM. Hits were marked as red rectangles in the plot and exact positions relative to the transcription start site (TSS) are reported below the plot. Motif libraries are from the JASPAR® database and the EPD elements and were downloaded as a text file(61). The description of the motifs and the conversion rules are shown in the figure. The scan of the motifs was performed on-the-fly using the FindM tool from the Signal Search Analysis server toolkit (https://ccg.epfl.ch/ssa/findm.php). We then only considered transcription factors which were detected after ethanol or ammonia treatment and were undetected in untreated samples. This resulted in 17 total transcription factors of interest. Using this data, we created a

Venn diagram of transcription factors bound in different conditions using the VennDiagram package in R.

Statistical analysis **-** Experimental data for all conditions are expressed as mean ± SEM and the number of animals used is provided in the figure legends. Quantitative variables were analyzed using the Student t-test for protocols with 2 groups. For all studies in which the experimental protocol involved more than 2 groups, data were analyzed using a one-way analysis of variance. When ANOVA showed a significant overall effect, differences among different groups were assessed using the Bonferroni post-hoc analysis. Qualitative variables were analyzed using the chi square test. A $p < 0.05$ was considered significant. All analyses were done using SPSS v20 (IBM, Armonk, NY, USA).

Acknowledgements: AMM is a Senior Research Associate from the FNRS and a WELBIO Investigator. Technical assistance and support were provided by Lakshmi Veera.

Conflict of interest: The authors declare that they have no conflicts of interest with the contents of this article.

Author contributions: SK, GD and SD designed, experiments performed, analyzed and interpreted the data, wrote the manuscript. KAA, AKu, NW, BW, DSL and MG: experiments performed, edited and reviewed manuscript. DW and AMM provided critical reagents and protocols, edited and reviewed manuscript. CH and VV performed experiments for alcohol and acetaldehyde dehydrogenase, edited and reviewed manuscript. AKi assisted with the bioinformatics analyses, assisted with the interpretation of data, edited and reviewed the manuscript. MM and LEN assisted with design and performed animal experiments, edited and reviewed manuscript.

References

1. Dasarathy, J., McCullough, A. J., and Dasarathy, S. (2017) Sarcopenia in Alcoholic Liver Disease: Clinical and Molecular Advances. *Alcohol Clin Exp Res* **41**, 1419-1431

2. Dasarathy, S. (2016) Nutrition and Alcoholic Liver Disease: Effects of Alcoholism on Nutrition, Effects of Nutrition on Alcoholic Liver Disease, and Nutritional Therapies for Alcoholic Liver Disease. *Clin Liver Dis* **20**, 535-550

3. Guirguis, J., Chhatwal, J., Dasarathy, J., Rivas, J., McMichael, D., Nagy, L. E., McCullough, A. J., and Dasarathy, S. (2015) Clinical impact of alcohol-related cirrhosis in the next decade: estimates based on current epidemiological trends in the United States. *Alcohol Clin Exp Res* **39**, 2085-2094

4. Thapaliya, S., Runkana, A., McMullen, M. R., Nagy, L. E., McDonald, C., Naga Prasad, S. V., and Dasarathy, S. (2014) Alcohol-induced autophagy contributes to loss in skeletal muscle mass. *Autophagy* **10**, 677-690

5. Fernandez-Sola, J., Preedy, V. R., Lang, C. H., Gonzalez-Reimers, E., Arno, M., Lin, J. C., Wiseman, H., Zhou, S., Emery, P. W., Nakahara, T., Hashimoto, K., Hirano, M., Santolaria-Fernandez, F., Gonzalez-Hernandez, T., Fatjo, F., Sacanella, E., Estruch, R., Nicolas, J. M., and Urbano-Marquez, A. (2007) Molecular and cellular events in alcohol-induced muscle disease. *Alcohol Clin Exp Res* **31**, 1953-1962

6. Nakahara, T., Hunter, R., Hirano, M., Uchimura, H., McArdle, A., Broome, C. S., Koll, M., Martin, C. R., and Preedy, V. R. (2006) Alcohol alters skeletal muscle heat shock protein gene expression in rats: these effects are moderated by sex, raised endogenous acetaldehyde, and starvation. *Metabolism* **55**, 843-851

7. Preedy, V. R., Edwards, P., and Peters, T. J. (1991) Ethanol-induced reductions in skeletal muscle protein synthesis: use of the inhibitors of alcohol and aldehyde dehydrogenase. *Biochem Soc Trans* **19**, 167S

8. Pacy, P. J., Preedy, V. R., Peters, T. J., Read, M., and Halliday, D. (1991) The effect of chronic alcohol ingestion on whole body and muscle protein synthesis--a stable isotope study. *Alcohol Alcohol* **26**, 505-513

9. Steiner, J. L., Kimball, S. R., and Lang, C. H. (2016) Acute Alcohol-Induced Decrease in Muscle Protein Synthesis in Female Mice Is REDD-1 and mTOR-Independent. *Alcohol Alcohol* **51**, 242-250

10. Steiner, J. L., and Lang, C. H. (2015) Dysregulation of skeletal muscle protein metabolism by alcohol. *Am J Physiol Endocrinol Metab* **308**, E699-712

11. Hong-Brown, L. Q., Frost, R. A., and Lang, C. H. (2001) Alcohol impairs protein synthesis and degradation in cultured skeletal muscle cells. *Alcohol Clin Exp Res* **25**, 1373-1382

12. Lang, C. H., Kimball, S. R., Frost, R. A., and Vary, T. C. (2001) Alcohol myopathy: impairment of protein synthesis and translation initiation. *Int J Biochem Cell Biol* **33**, 457-473

13. Lang, C. H., Frost, R. A., Kumar, V., Wu, D., and Vary, T. C. (2000) Impaired protein synthesis induced by acute alcohol intoxication is associated with changes in eIF4E in muscle and eIF2B in liver. *Alcohol Clin Exp Res* **24**, 322-331

14. Lang, C. H., Wu, D., Frost, R. A., Jefferson, L. S., Kimball, S. R., and Vary, T. C. (1999) Inhibition of muscle protein synthesis by alcohol is associated with modulation of eIF2B and eIF4E. *Am J Physiol* **277**, E268-276

15. Lang, C. H., Pruznak, A. M., Deshpande, N., Palopoli, M. M., Frost, R. A., and Vary, T. C. (2004) Alcohol intoxication impairs phosphorylation of S6K1 and S6 in skeletal muscle independently of ethanol metabolism. *Alcohol Clin Exp Res* **28**, 1758-1767

16. Marway, J. S., and Preedy, V. R. (1995) The acute effects of ethanol and acetaldehyde on the synthesis of mixed and contractile proteins of the jejunum. *Alcohol Alcohol* **30**, 211-217

17. Preedy, V. R., Keating, J. W., and Peters, T. J. (1992) The acute effects of ethanol and acetaldehyde on rates of protein synthesis in type I and type II fibre-rich skeletal muscles of the rat. *Alcohol Alcohol* **27**, 241-251

18. Cederbaum, A. I. (2012) Alcohol metabolism. *Clin Liver Dis* **16**, 667-685

19. Lang, C. H., Frost, R. A., Summer, A. D., and Vary, T. C. (2005) Molecular mechanisms responsible for alcohol-induced myopathy in skeletal muscle and heart. *Int J Biochem Cell Biol* **37**, 2180-2195

20. Aagaard, N. K., Thogersen, T., Grofte, T., Greisen, J., and Vilstrup, H. (2004) Alcohol acutely down-regulates urea synthesis in normal men. *Alcohol Clin Exp Res* **28**, 697-701

21. Glavind, E., Aagaard, N. K., Gronbaek, H., Orntoft, N. W., Vilstrup, H., and Thomsen, K. L. (2017) Time course of compromised urea synthesis in patients with alcoholic hepatitis. *Scand J Gastroenterol*, 1-6

22. Schricker, T., Albuszies, G., Weidenbach, H., Beckh, K. H., Ensinger, H., Geisser, W., Adler, G., and Georgieff, M. (1997) [Liver urea and glucose production in patients with alcohol-induced cirrhosis]. *Dtsch Med Wochenschr* **122**, 75-79

23. Maier, K. P., Volk, B., Hoppe-Seyler, G., and Gerok, W. (1974) Urea-cycle enzymes in normal liver and in patients with alcoholic hepatitis. *Eur J Clin Invest* **4**, 193-195

24. Olde Damink, S. W., Jalan, R., and Dejong, C. H. (2009) Interorgan ammonia trafficking in liver disease. *Metab Brain Dis* **24**, 169-181

25. Rypins, E. B., Henderson, J. M., Fulenwider, J. T., Moffitt, S., Galambos, J. T., Warren, W. D., and Rudman, D. (1980) A tracer method for measuring rate of urea synthesis in normal and cirrhotic subjects. *Gastroenterology* **78**, 1419-1424

26. Rudman, D., DiFulco, T. J., Galambos, J. T., Smith, R. B., 3rd, Salam, A. A., and Warren, W. D. (1973) Maximal rates of excretion and synthesis of urea in normal and cirrhotic subjects. *J Clin Invest* **52**, 2241-2249

27. Holmuhamedov, E. L., Czerny, C., Beeson, C. C., and Lemasters, J. J. (2012) Ethanol suppresses ureagenesis in rat hepatocytes: role of acetaldehyde. *J Biol Chem* **287**, 7692-7700

28. Dasarathy, S., and Hatzoglou, M. (2018) Hyperammonemia and proteostasis in cirrhosis. *Curr Opin Clin Nutr Metab Care* **21**, 30-36

29. Qiu, J., Thapaliya, S., Runkana, A., Yang, Y., Tsien, C., Mohan, M. L., Narayanan, A., Eghtesad, B., Mozdziak, P. E., McDonald, C., Stark, G. R., Welle, S., Naga Prasad, S. V., and Dasarathy, S. (2013) Hyperammonemia in cirrhosis induces transcriptional regulation of myostatin by an NF-kappaB-mediated mechanism. *Proc Natl Acad Sci U S A* **110**, 18162-18167

30. Lockwood, A. H., McDonald, J. M., Reiman, R. E., Gelbard, A. S., Laughlin, J. S., Duffy, T. E., and Plum, F. (1979) The dynamics of ammonia metabolism in man. Effects of liver disease and hyperammonemia. *J Clin Invest* **63**, 449-460

31. Kumar, A., Davuluri, G., Silva, R. N. E., Engelen, M., Ten Have, G. A. M., Prayson, R., Deutz, N. E. P., and Dasarathy, S. (2017) Ammonia lowering reverses sarcopenia of cirrhosis by restoring skeletal muscle proteostasis. *Hepatology* **65**, 2045-2058

32. Dasarathy, S., Mookerjee, R. P., Rackayova, V., Rangroo Thrane, V., Vairappan, B., Ott, P., and Rose, C. F. (2017) Ammonia toxicity: from head to toe? *Metab Brain Dis* **32**, 529-538

33. Davuluri, G., Krokowski, D., Guan, B. J., Kumar, A., Thapaliya, S., Singh, D., Hatzoglou, M., and Dasarathy, S. (2016) Metabolic adaptation of skeletal muscle to hyperammonemia drives the beneficial effects of l-leucine in cirrhosis. *J Hepatol* **65**, 929-937

34. McDaniel, J., Davuluri, G., Hill, E. A., Moyer, M., Runkana, A., Prayson, R., van Lunteren, E., and Dasarathy, S. (2016) Hyperammonemia results in reduced muscle function independent of muscle mass. *Am J Physiol Gastrointest Liver Physiol* **310**, G163-170

35. Stern, R. A., Ashwell, C. M., Dasarathy, S., and Mozdziak, P. E. (2015) The effect of hyperammonemia on myostatin and myogenic regulatory factor gene expression in broiler embryos. *Animal* **9**, 992-999

36. Qiu, J., Tsien, C., Thapalaya, S., Narayanan, A., Weihl, C. C., Ching, J. K., Eghtesad, B., Singh, K., Fu, X., Dubyak, G., McDonald, C., Almasan, A., Hazen, S. L., Naga Prasad, S. V., and Dasarathy, S. (2012) Hyperammonemia-mediated autophagy in skeletal muscle contributes to sarcopenia of cirrhosis. *Am J Physiol Endocrinol Metab* **303**, E983-993

37. Takeda, K., and Takemasa, T. (2015) Expression of ammonia transporters Rhbg and Rhcg in mouse skeletal muscle and the effect of 6-week training on these proteins. *Physiol Rep* **3**

38. Weiner, I. D., and Verlander, J. W. (2003) Renal and hepatic expression of the ammonium transporter proteins, Rh B Glycoprotein and Rh C Glycoprotein. *Acta Physiol Scand* **179**, 331-338

39. Hershey, J. W., Sonenberg, N., and Mathews, M. B. (2012) Principles of translational control: an overview. *Cold Spring Harb Perspect Biol* **4**

40. Merhi, A., De Mees, C., Abdo, R., Victoria Alberola, J., and Marini, A. M. (2015) Wnt/beta-Catenin Signaling Regulates the Expression of the Ammonium Permease Gene RHBG in Human Cancer Cells. *PLoS One* **10**, e0128683

41. Inostroza, J. A., Mermelstein, F. H., Ha, I., Lane, W. S., and Reinberg, D. (1992) Dr1, a TATA-binding protein-associated phosphoprotein and inhibitor of class II gene transcription. *Cell* **70**, 477-489

42. Yeung, K. C., Inostroza, J. A., Mermelstein, F. H., Kannabiran, C., and Reinberg, D. (1994) Structure-function analysis of the TBP-binding protein Dr1 reveals a mechanism for repression of class II gene transcription. *Genes Dev* **8**, 2097-2109

43. Xue, Y., Pradhan, S. K., Sun, F., Chronis, C., Tran, N., Su, T., Van, C., Vashisht, A., Wohlschlegel, J., Peterson, C. L., Timmers, H. T. M., Kurdistani, S. K., and Carey, M. F. (2017) Mot1, Ino80C, and NC2 Function Coordinately to Regulate Pervasive Transcription in Yeast and Mammals. *Mol Cell* **67**, 594-607 e594

44. Maier, K. P., Talke, H., Heimsoeth, H., and Gerok, W. (1978) Influence of steroids on urea-cycle enzymes in chronic human liver disease. *Klin Wochenschr* **56**, 291-295

45. Molina, P. E., Lang, C. H., McNurlan, M., Bagby, G. J., and Nelson, S. (2008) Chronic alcohol accentuates simian acquired immunodeficiency syndrome-associated wasting. *Alcohol Clin Exp Res* **32**, 138-147

46. Reilly, M. E., Preedy, V. R., and Peters, T. J. (1995) Investigations into the toxic effects of alcohol on skeletal muscle. *Adverse Drug React Toxicol Rev* **14**, 117-150

47. Steiner, J. L., and Lang, C. H. (2014) Alcohol impairs skeletal muscle protein synthesis and mTOR signaling in a time-dependent manner following electrically stimulated muscle contraction. *J Appl Physiol (1985)* **117**, 1170-1179

48. Hong-Brown, L. Q., Brown, C. R., Huber, D. S., and Lang, C. H. (2007) Alcohol regulates eukaryotic elongation factor 2 phosphorylation via an AMP-activated protein kinase-dependent mechanism in C2C12 skeletal myocytes. *J Biol Chem* **282**, 3702-3712

49. Liangpunsakul, S., Sozio, M. S., Shin, E., Zhao, Z., Xu, Y., Ross, R. A., Zeng, Y., and Crabb, D. W. (2010) Inhibitory effect of ethanol on AMPK phosphorylation is mediated in part through elevated ceramide levels. *Am J Physiol Gastrointest Liver Physiol* **298**, G1004-1012

50. Dasarathy, S., and Merli, M. (2016) Sarcopenia from mechanism to diagnosis and treatment in liver disease. *J Hepatol* **65**, 1232-1244

51. Verlander, J. W., Miller, R. T., Frank, A. E., Royaux, I. E., Kim, Y. H., and Weiner, I. D. (2003) Localization of the ammonium transporter proteins RhBG and RhCG in mouse kidney. *Am J Physiol Renal Physiol* **284**, F323-337

52. Mak, D. O., Dang, B., Weiner, I. D., Foskett, J. K., and Westhoff, C. M. (2006) Characterization of ammonia transport by the kidney Rh glycoproteins RhBG and RhCG. *Am J Physiol Renal Physiol* **290**, F297-305

53. Davuluri, G., Allawy, A., Thapaliya, S., Rennison, J. H., Singh, D., Kumar, A., Sandlers, Y., Van Wagoner, D. R., Flask, C. A., Hoppel, C., Kasumov, T., and Dasarathy, S. (2016) Hyperammonaemia-induced skeletal muscle mitochondrial dysfunction results in cataplerosis and oxidative stress. *J Physiol* **594**, 7341-7360

54. Bakhautdin, B., Das, D., Mandal, P., Roychowdhury, S., Danner, J., Bush, K., Pollard, K., Kaspar, J. W., Li, W., Salomon, R. G., McMullen, M. R., and Nagy, L. E. (2014) Protective role of HO-1 and carbon monoxide in ethanol-induced hepatocyte cell death and liver injury in mice. *J Hepatol* **61**, 1029-1037

55. Tsien, C., Davuluri, G., Singh, D., Allawy, A., Ten Have, G. A., Thapaliya, S., Schulze, J. M., Barnes, D., McCullough, A. J., Engelen, M. P., Deutz, N. E., and Dasarathy, S. (2015) Metabolic and molecular responses to leucine-enriched branched chain amino acid supplementation in the skeletal muscle of alcoholic cirrhosis. *Hepatology* **61**, 2018-2029

56. Schneider, C. A., Rasband, W. S., and Eliceiri, K. W. (2012) NIH Image to ImageJ: 25 years of image analysis. *Nat Methods* **9**, 671-675

57. Zawada, R. J., Kwan, P., Olszewski, K. L., Llinas, M., and Huang, S. G. (2009) Quantitative determination of urea concentrations in cell culture medium. *Biochem Cell Biol* **87**, 541-544

58. Tyanova, S., Temu, T., and Cox, J. (2016) The MaxQuant computational platform for mass spectrometry-based shotgun proteomics. *Nat Protoc* **11**, 2301-2319

59. Cox, J., and Mann, M. (2008) MaxQuant enables high peptide identification rates, individualized p.p.b.-range mass accuracies and proteome-wide protein quantification. *Nat Biotechnol* **26**, 1367-1372

60. Cox, J., Hein, M. Y., Luber, C. A., Paron, I., Nagaraj, N., and Mann, M. (2014) Accurate proteome-wide label-free quantification by delayed normalization and maximal peptide ratio extraction, termed MaxLFQ. *Mol Cell Proteomics* **13**, 2513-2526

61. Dreos, R., Ambrosini, G., Cavin Perier, R., and Bucher, P. (2013) EPD and EPDnew, high-quality promoter resources in the next-generation sequencing era. *Nucleic Acids Res* **41**, D157-164

FOOTNOTES

Funded in part by R21 AA022742 (SD, GD); RO1 GM119174; RO1 DK113196 (SD); P50 AA024333 (LN, SD); UO1 AA021890 (LN, SD), RO1 DK045788 (IDW), RO1 KB107798 (IDW), UO1 AA021724 (VV), R24 AA022057 (VV) and the Mikati Foundation Grant support to (SD and GD).

The abbreviations used are: ADH, alcohol dehydrogenase; ALDH, aldehyde dehydrogenase; AMPK, adenosine monophosphate–activated protein kinase; EF, Ethanol fed; eIF, eukaryotic initiation factor; GCN, general control non-derepressible; mTORC1, mammalian target of rapamycin complex 1; PERK Protein kinase RNA activated like endoplasmic reticulum kinase; PF, pair-fed.

Figure.1

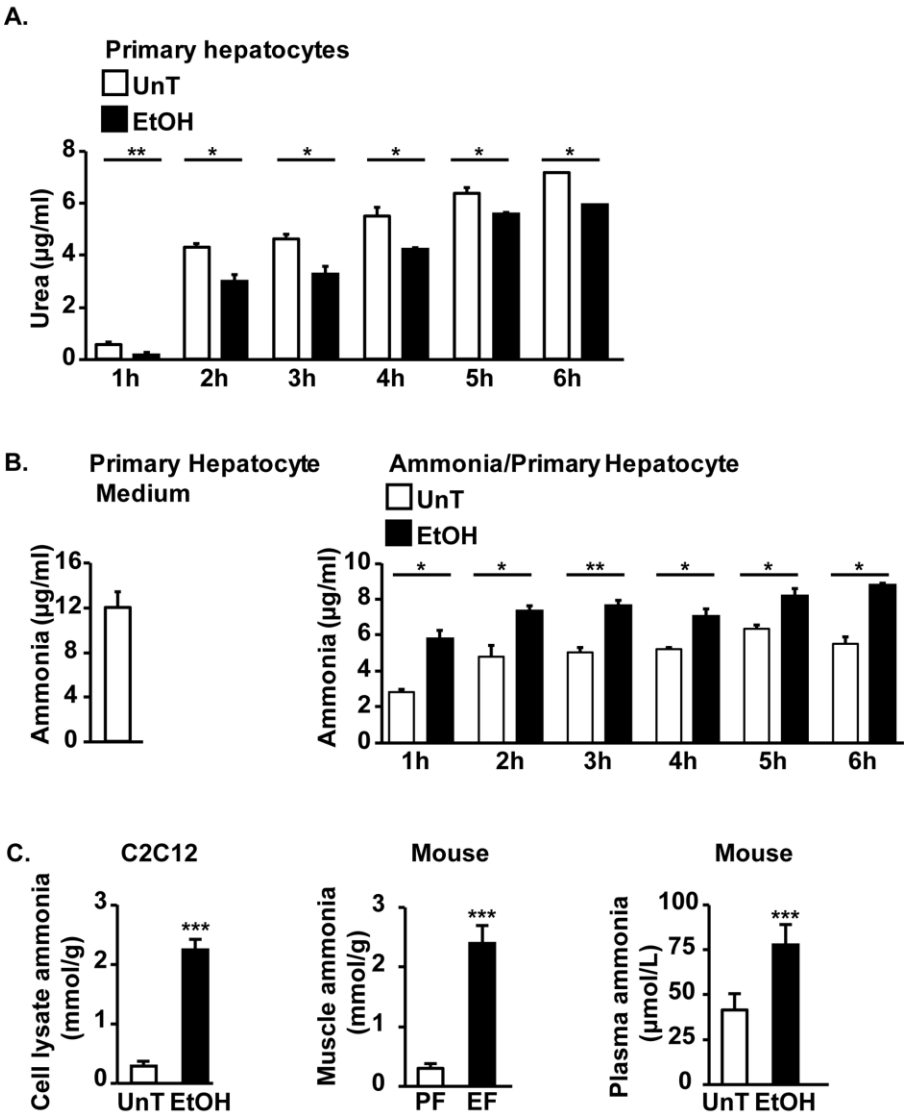

Fig. 1. **Ethanol exposure impairs ureagenesis in primary hepatocyte and increases plasma and muscle ammonia concentrations**. **Panel A, B**. Concentrations of urea and ammonia in the medium from murine primary hepatocytes treated for different time points with 100mM ethanol. **Panel C**. Ammonia concentration in plasma and skeletal muscle from ethanol or pair fed mice and myotubes treated with 100mM ethanol for 24h. Data are expressed as mean ± S.E.M from at least 3 biological replicates. *p < 0.05, **p < 0.01, ***p < 0.001 vs. untreated controls.

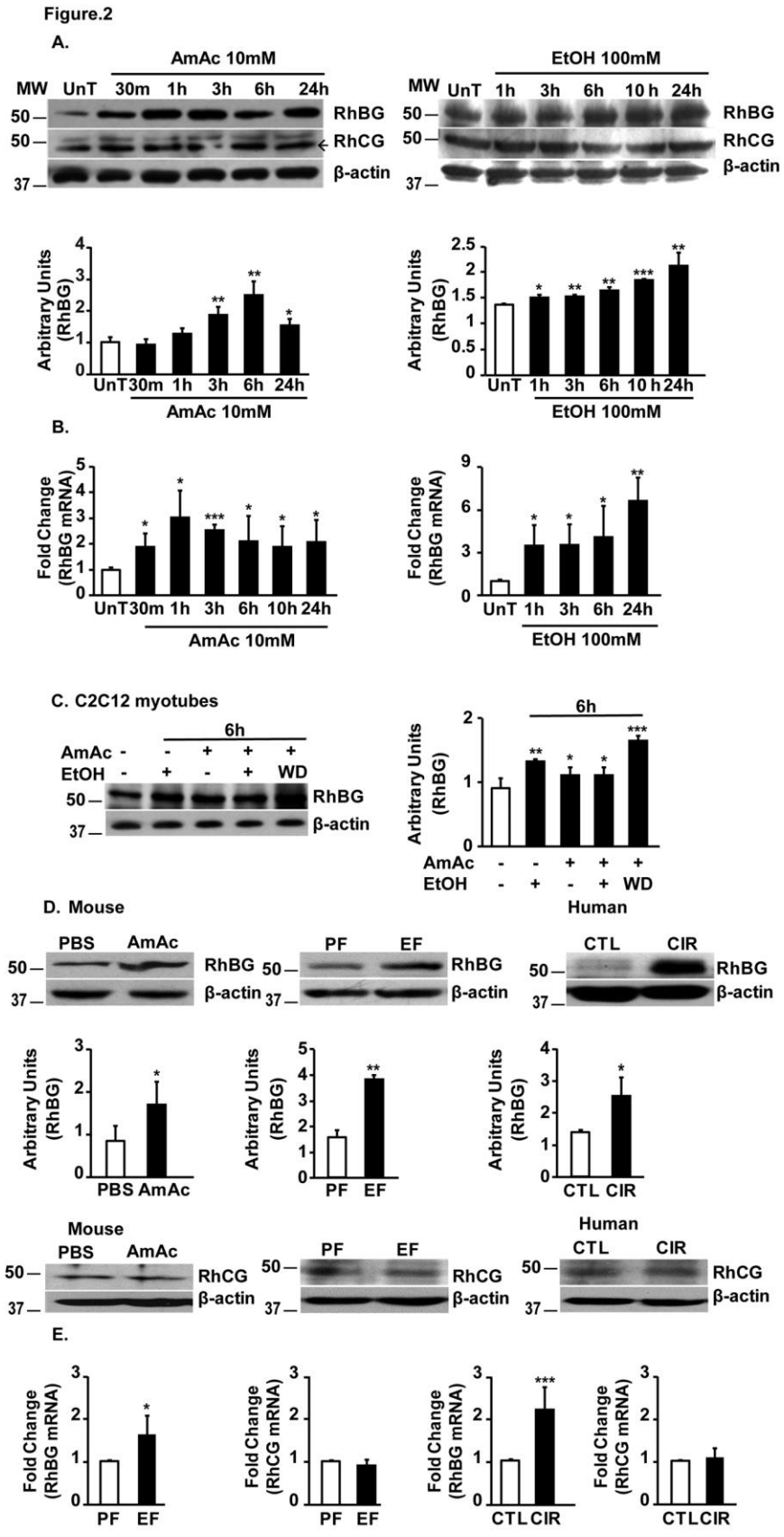

Fig. 2. Ethanol and hyperammonemia independently increase skeletal muscle RhBG expression. Panel A. Representative immunoblots and densitometry for ammonia transporters, RhBG and RhCG, in C2C12 myotubes treated with 10mM ammonium acetate or 100mM ethanol for different time points. **Panel B**. Fold change in expression of RhBG mRNA by real time PCR in C2C12 myotubes treated with 10mM ammonium acetate or 100mM ethanol for different time points. **Panel C**. Representative immunoblots and densitometry of ammonia transporter, RhBG, expression in murine C2C12 myotubes treated with 100mM ethanol, 10mM ammonium acetate, both or 10mM ammonium acetate for 6h after ethanol withdrawal. **Panel D**. Representative immunoblots and densitometry of RhBG expression and representative immunoblots of RhCG expression in gastrocnemius muscle from hyperammonemic and control (n=3 each), chronic ethanol and pair fed mice (n=3 each) and skeletal muscle from patients with cirrhosis and control subjects (n=4 each). **Panel E**. Fold change in expression of ammonia transporters, RhBG mRNA and RhCG mRNA by real time PCR, in chronic ethanol or pair fed mice (n=3 each) and patients with alcoholic cirrhosis and controls (n=4 each). All data expressed as mean±SD. * $p<0.05$; ** $p<0.01$; *** $p<0.001$ vs. controls.

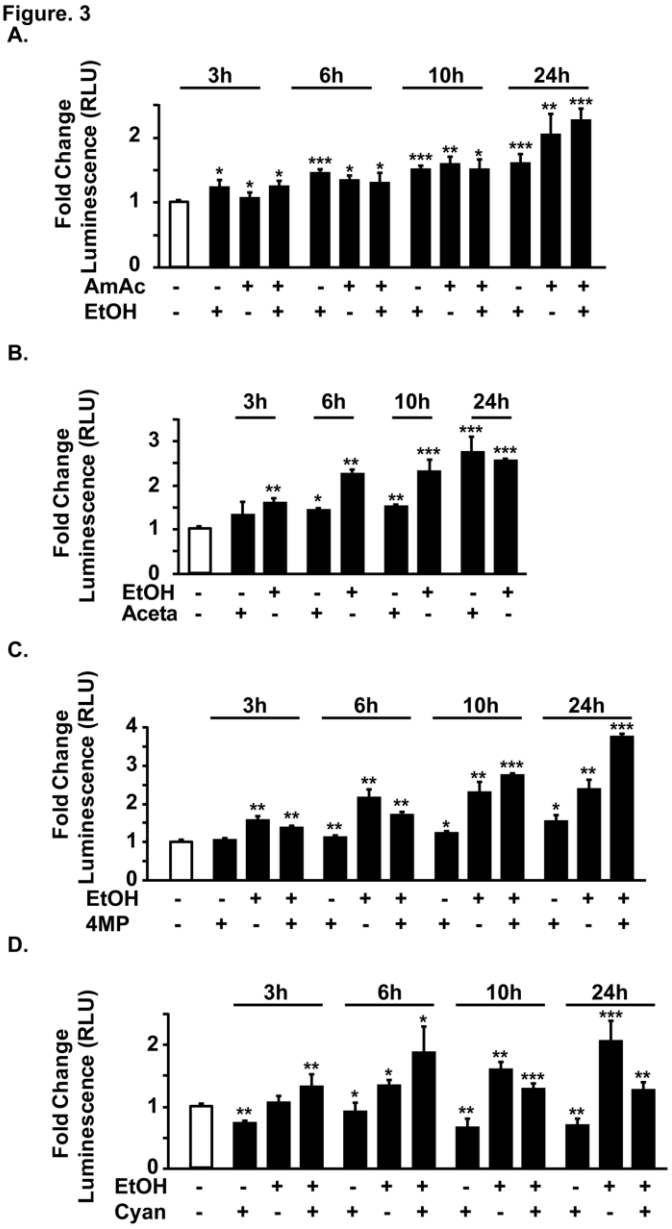

Fig. 3. Transcriptional upregulation of RhBG by ethanol and hyperammonemia. Murine C2C12 cells transfected with the empty plasmid (pGL3) or RhBG promoter (pGL3-RhBG) with Renilla plasmid and differentiated to myotubes and treated as below with different interventions for stated times. Data expressed as relative luciferase units of luminescence of luciferase/Renilla. **Panel A**. RhBG transcriptional response by reporter assay in response to 10mM ammonium acetate, 100mM ethanol or both. **Panel B**. Response of RhBG reporter in to 100mM ethanol or 1mM acetaldehyde. **Panel C**. Response of RhBG reporter to 100mM ethanol with and without 1mM 4-methylpyrazole, an alcohol dehydrogenase inhibitor. **Panel D**. Response of RhBG reporter in to 100mM ethanol with and without 0.3mM cyanamide, an acetaldehyde dehydrogenase inhibitor. All data from at least 3 biological replicates expressed as mean ± S.E.M of the pGL3-RhBG luciferase activity relative to pGL3-Basic. EtOH, Ethanol; AmAc, Ammonium acetate; Aceta, Acetaldehyde; Cyana, Cyanamide; 4-MP, 4-methylpyrazole. *$p < 0.05$, **$p < 0.01$, ***$p < 0.001$ vs. untreated controls.

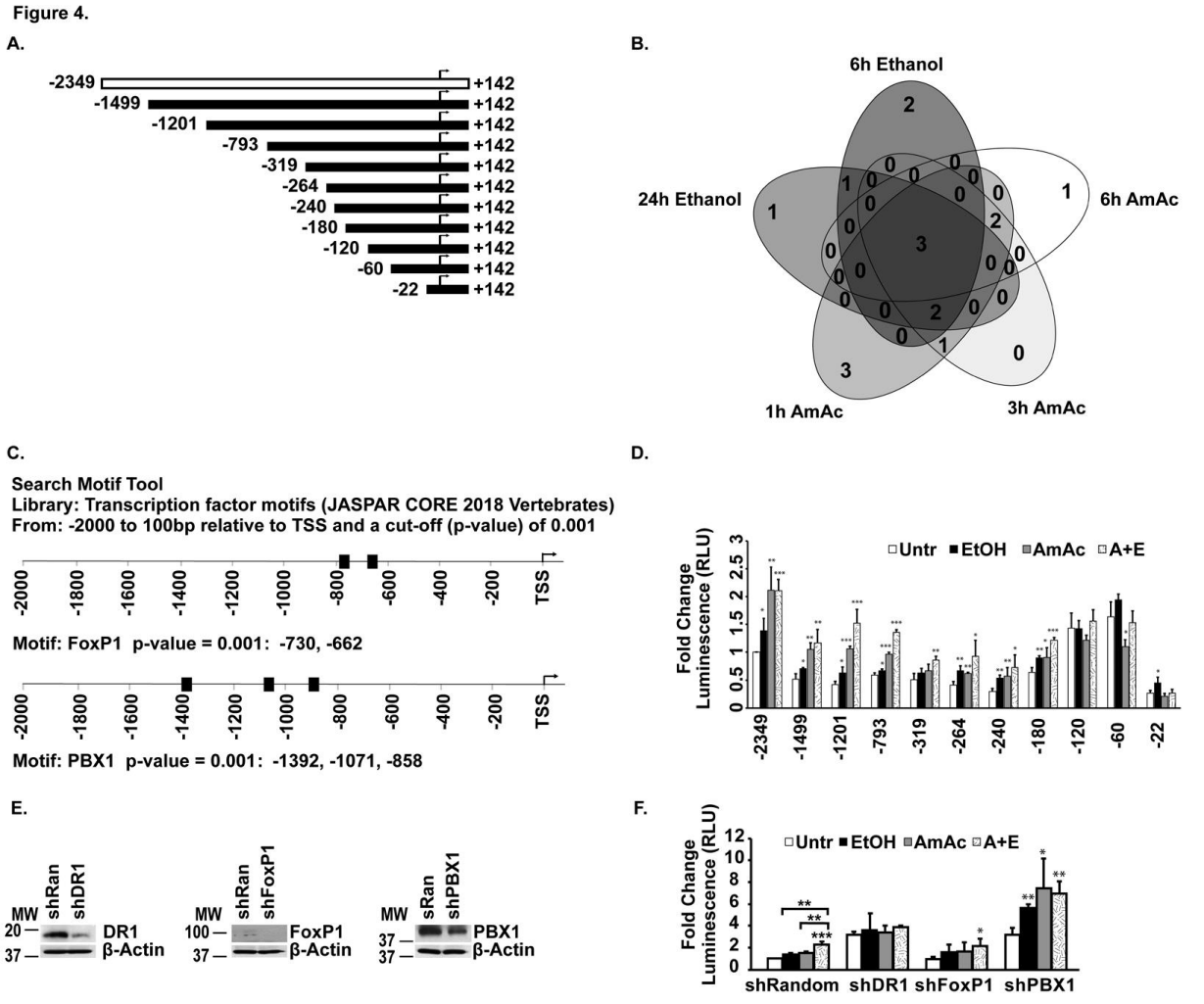

Fig. 4. **Regulation of RhBG promoter in response to ethanol and hyperammonemia. Panel A.** RhBG full length and deletion constructs were cloned in pGL3 basic vector. Arrow denotes transcription start site (TSS). **Panel B.** Venn diagram of transcription factors bound to full length RhBG promoter in response to 10mM ammonium acetate (AmAc) or 100mM ethanol for stated times in hours (h) identified by proteomics from biotin tagged full length promoter pulldown assay. **Panel C**. Bioinformatics analysis of the RhBG promoter to identify consensus sequences for the transcription factors that were identified by promoter pulldown assay. **Panel D**. Reporter assay in C2C12 myoblasts transfected with full length RhBG promoter or the indicated construct subcloned in pGL3 with Renilla plasmid. Luciferase activity with no treatment (Untr). 24 h treatment with 100mM ethanol (EtOH), 10mM ammonium acetate (AmAc) or both ethanol and ammonium acetate. All data expressed as fold change compared to untreated control cells. **Panel E**. Representative immunoblots of the 3 transcription factors that were bound to the RhBG promoter in C2C12 myotubes with mock or shRNA transfection. **Panel F**. Reporter activity of full length RhBG promoter in myotubes with silencing of DR1, FoxP1 and PBX1 in response to 100mM ethanol, 10mM ammonium acetate or both for 24h. Luciferase activity expressed as fold change compared to untreated control cells for each group (shRandom, shDR1, shFoxP1, shPBX1). Data are expressed as mean of at least three biological replicates expressed mean ± S.E.M of the pGL3-RhBG construct normalized with Renilla response. * $p<0.05$; ** $p<0.01$; *** $p<0.001$.

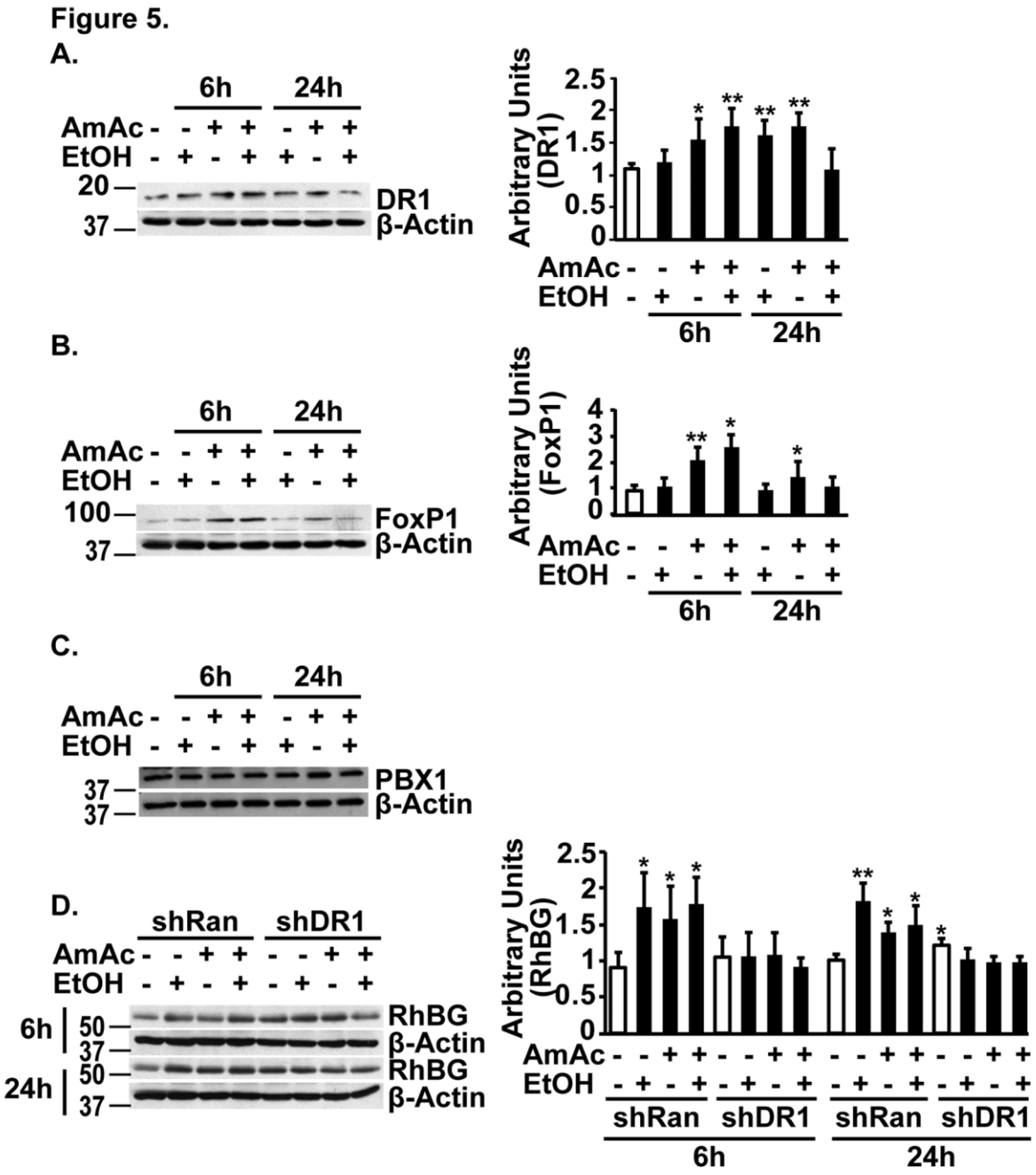

Fig. 5. Expression of transcription factors in response to ethanol or ammonia. Panels A-C. Representative immunoblots and densitometry of transcription factor Dr1 and FoxP1 and immunoblots of PBX1 in murine C2C12 myotubes treated with 100mM ethanol (EtOH), 10mM ammonium acetate (AmAc) or both EtOH and AmAc for 6 and 24 h. **Panel D**. Representative immunoblots and densitometry of RhBG protein in C2C12 myotubes with either mock transfection or shDR1 treated with 100mM ethanol (EtOH), 10mM ammonium acetate (AmAc) or both for 6 and 24h. All data expressed as mean±SD from at least 3 biological replicates. *p <0.05, **p < 0.01, ***p < 0.001.

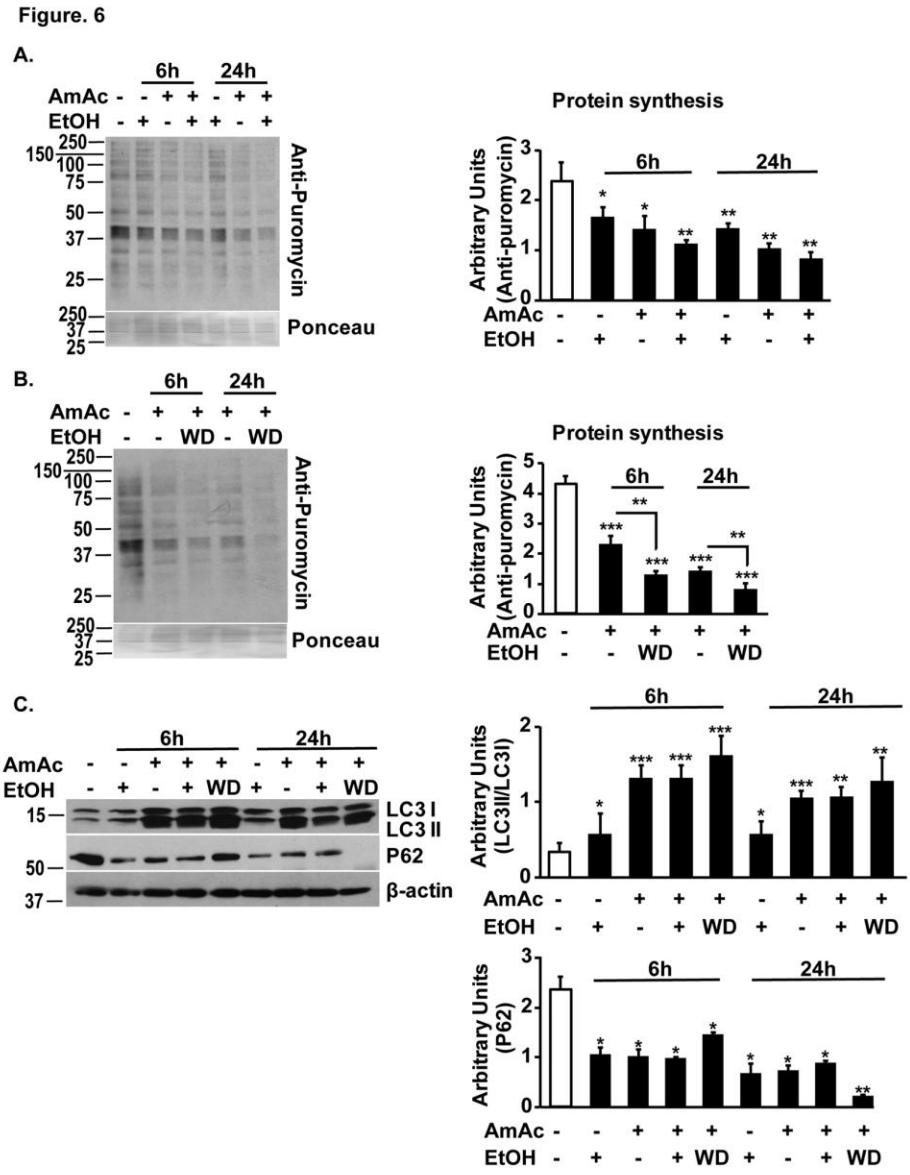

Fig. 6. Ethanol and hyperammonemia independently cause dysregulated proteostasis. Panel A. Representative immunoblots and densitometry (from the entire lane) for puromycin incorporation in murine C2C12 myotubes treated with 100mM ethanol, 10mM ammonium acetate or both for 6 and 24 h. **Panel B.** Representative immunoblots and densitometry for puromycin incorporation in murine C2C12 myotubes in response to treatment with 10mM ammonium acetate following withdrawal of 100mM ethanol. **Panel C.** Representative immunoblots and densitometries of LC3 lipidation and P62 showed increased autophagy in response to 10mM ammonium acetate treatment for 6 and 24h following withdrawal of 100mM ethanol. Treatment with ethanol alone showed less autophagy compared with ethanol with hyperammonemia or hyperammonemia following ethanol withdrawal. All myotube data from at least 3 biological replicates. EtOH, Ethanol; AmAc, Ammonium Acetate; WD, Ethanol withdrawal followed by ammonium acetate treatment. *p < 0.05, **p < 0.01, ***p < 0.001 vs. untreated controls.

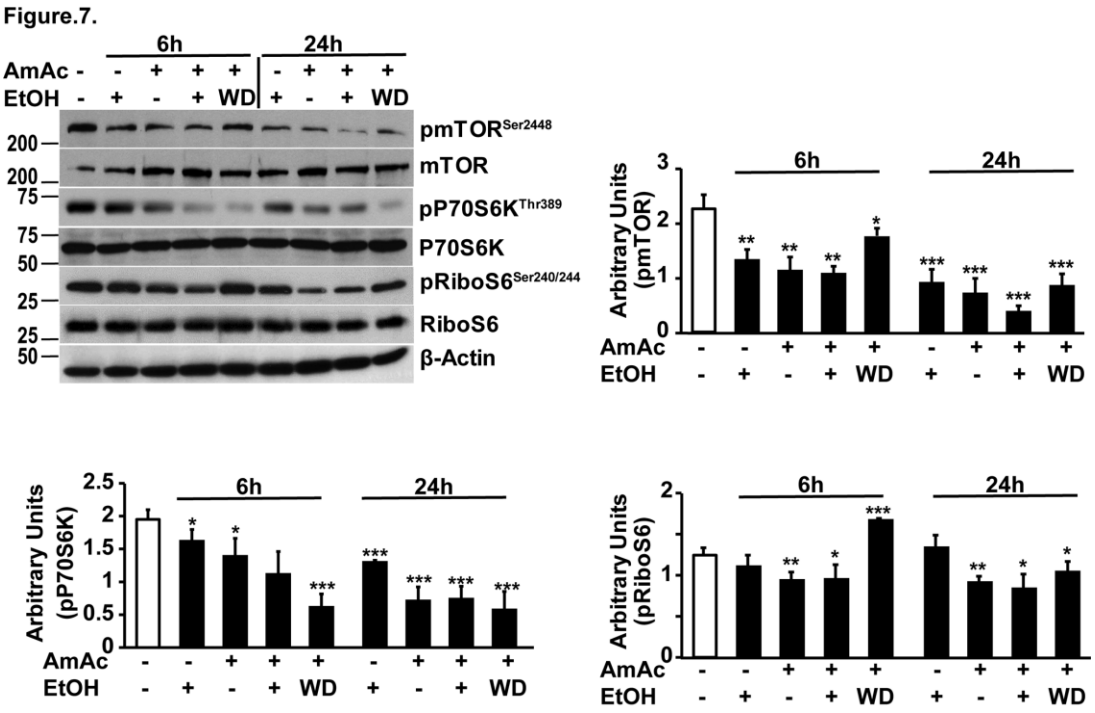

Fig.7. Impaired mTORC1 signaling in C2C12 myotubes during ethanol treatment and hyperammonemia. Representative immunoblots and densitometry of phosphorylated mTOR (Ser^{2448}) and signaling response to mTORC1 activation (phosphorylation of P70S6 kinase and ribosomal S6 protein) in murine C2C12 myotubes treated with 100mM ethanol, 10mM ammonium acetate, both ethanol and ammonium acetate or 10mM ammonium acetate following ethanol withdrawal for stated time points. EtOH, 100mM ethanol; AmAc, 10mM ammonium acetate; WD, Ethanol withdrawal followed by 10mM ammonium acetate treatment. All data expressed as mean±SD from at least 3 biological replicates. *p < 0.05, **p < 0.01, ***p < 0.001 vs. untreated controls.

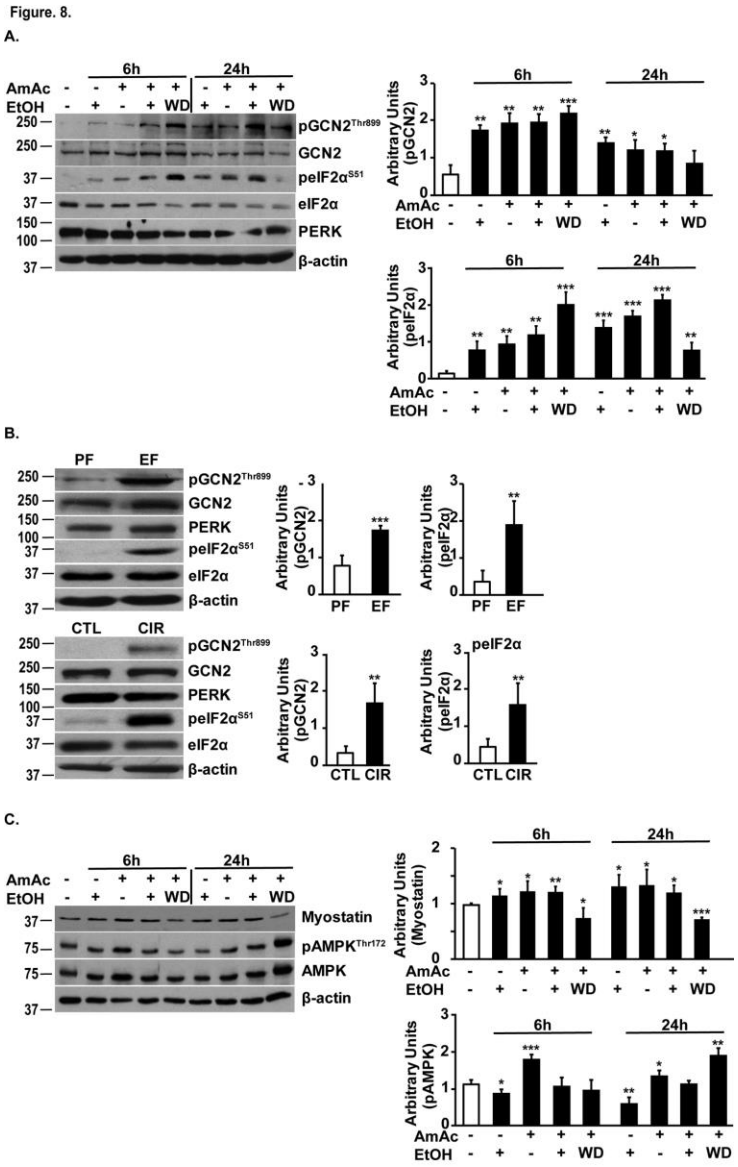

Fig. 8. Ethanol and ammonia result in phosphorylation of eIF2α and AMPK. Panel A. Representative immunoblots and densitometry of phosphorylated GCN2 and eIF2α in murine C2C12 myotubes exposure to 100mM ethanol, 10mM ammonium acetate, both ethanol and ammonium acetate, or 10mM ammonium acetate following withdrawal of 100mM ethanol for 6 and 24h. No PERK activation as determined by lack of mobility shift on electrophoresis. **Panel B**. Representative immunoblots and densitometry of phosphorylated GCN2, eIF2α and no PERK activation as determined by lack of mobility shift in gastrocnemius muscle from ethanol and pair fed mice (n=3 each) and skeletal muscle from patients with alcoholic cirrhosis and controls (n=3 each). **Panel C.** Representative immunoblots and densitometry of myostatin and phospho-AMPK in myotubes treated with 100mM ethanol or 10mM ammonium acetate alone, both ethanol and ammonium acetate and 10mM ammonium acetate following ethanol withdrawal for 6 and 24h . EtOH, Ethanol; AmAc, Ammonium Acetate; WD, Ethanol withdrawal followed by ammonium acetate treatment. All data expressed as mean±SD. Densitometry determined from at least 3 biological replicates for studies in myotubes. *p < 0.05, **p < 0.01, ***p < 0.001 vs. controls.

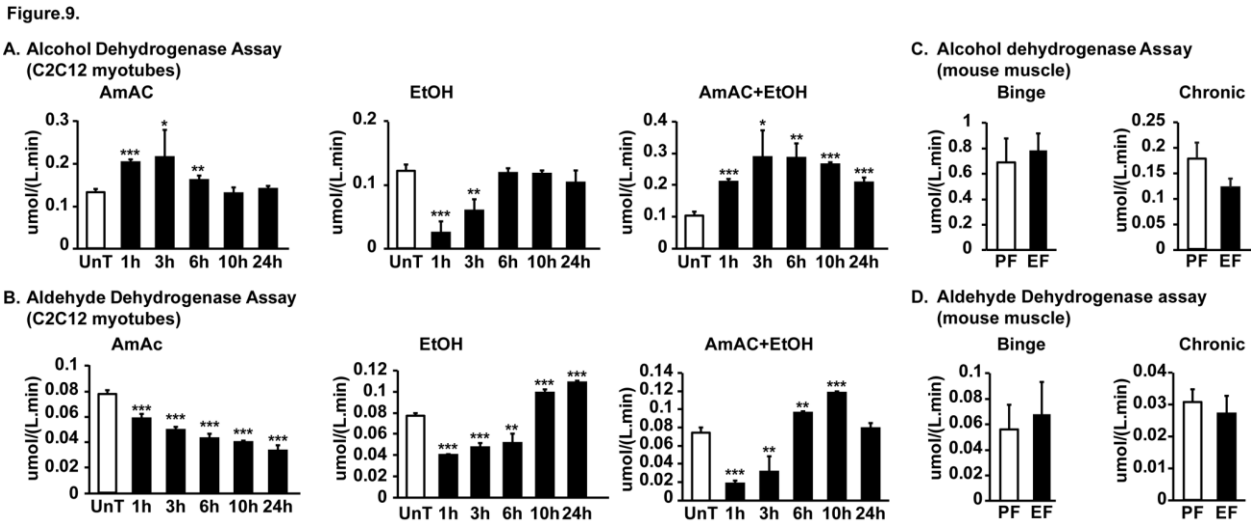

Fig. 9. Skeletal muscle expression and activity of ethanol metabolizing enzymes. Panels A, B. C2C12 myotubes were treated with 100mM ethanol, 10mM ammonium acetate, and in combination of ethanol and ammonium acetate for stated times. Alcohol dehydrogenase (ADH) and aldehyde dehydrogenase activities (ALDH) activities were quantified. **Panel C, D**. Alcohol and aldehyde dehydrogenase activity assays in gastrocnemius muscle from mice treated with chronic or binge ethanol or pair fed mice (n=4 each). All myotube experiments were done in three biological replicates. All data expressed mean ± SD. *p < 0.05, **p < 0.01, ***p < 0.001 vs. controls.

Ethanol sensitizes skeletal muscle to ammonia-induced molecular perturbations

Sashi Kant, Gangarao Davuluri, Khaled A. Alchirazi, Nicole Welch, Claire Heit, Avinash Kumar, Mahesha Gangadhariah, Adam Kim, Megan R. McMullen, Belinda Willard, Donal S. Luse, Laura E. Nagy, Vasilis Vasiliou, Anna Maria Marini, David Weiner and Srinivasan Dasarathy

J. Biol. Chem. published online March 14, 2019
